

The Preventive Destruction of a Hazardous Asteroid

A. G. Aleksandrova^{1*}, T. Yu. Galushina¹, A. B. Prishchepenko²,
K. V. Kholshchikov^{1,3}, and V. M. Chechetkin^{1,4}

¹Tomsk State University, Tomsk, Russia

²“Sirius” Scientific Research and Experimental Center, Moscow, Russia

³St. Petersburg State University, St. Petersburg, Russia

⁴Keldysh Institute of Applied Mathematics, Russian Academy of Sciences, Moscow, Russia

Received June 23, 2015; in final form, October 20, 2015

Abstract—One means of countering a hazardous asteroid is discussed: destruction of the object using a nuclear charge. Explosion of such an asteroid shortly before its predicted collision would have catastrophic consequences, with numerous highly radioactive fragments falling onto the Earth. The possibility of exploding the asteroid several years before its impact is also considered. Such an approach is made feasible because the vast majority of hazardous objects pass by the Earth several times before colliding with it. Computations show that, in the 10 years following the explosion, only a negligible number of fragments fall onto the Earth, whose radioactivity has substantially reduced during this time. In most cases, none of these fragments collides with the Earth. Thus, this proposed method for eliminating a threat from space is reasonable in at least two cases: when it is not possible to undergo a soft removal of the object from the collisional path, and to destroy objects that are continually returning to near-Earth space and require multiple removals from hazardous orbits.

DOI: 10.1134/S1063772916040016

1. INTRODUCTION

The reality of the danger posed by asteroids is now widely recognized [1]. Several means of countering hazardous asteroids have been proposed, each of which has its advantages and disadvantages. The most radical of these is explosion with a nuclear device, with the aim of destroying the hazardous celestial body [2–4]. This option is usually proposed for the final interval of the asteroid’s trajectory, several months before its impact on the Earth. The main disadvantage of this approach is that a collection of highly radioactive fragments would then fall onto the planet.

In our current study, we consider the explosion of an asteroid several years before its predicted impact. This approach is made feasible by the fact that a collision with an asteroid with a diameter of 100 m or more just after its discovery is unlikely. Fortunately, the collision with the Earth itself is also unlikely. The estimated collision rate is one event roughly every 2000 yrs [5, 6]. The probability of impact just after the discovery of a hazardous object is two to three orders

of magnitude lower still.¹ In general, such a body will pass near the Earth several times (and thus be discovered) before it finally collides with the Earth [7, 8]. The preventive destruction of such an object long before its ultimate collision means that nearly all the blast fragments move away from the collisional orbit.

2. DESTRUCTION OF A HAZARDOUS ASTEROID

Let us take an asteroid \mathcal{A} to be a homogeneous ball with diameter D and density ρ . We will assume that it consists of a material such as monolithic granite (with initial density $\rho = 2500 \text{ kg/m}^3$ and nuclear pressures for vaporization and melting of 0.15 and 0.068 TPa, respectively), and that the fragments that result from the explosion are comparatively harmless, having characteristic sizes of no more than 10 m.

Real asteroids have irregular shapes and can be both more rigid (metallic asteroids such as Asteroid 6178) and less rigid (partially fragmented asteroids such as Asteroid 17656 Hayabusa). However, our

¹ This is not true for bodies with diameters of meters to tens of meters, which are detected only in the immediate vicinity of the Earth. However, the destruction or deflection of such bodies does not require nuclear charges.

*E-mail: tanast@nxt.ru

goal is to provide a qualitative picture of this approach in order to estimate its effectiveness, and the adopted idealization of the model problem is admissible.

We have studied the explosion of a nuclear device with an energy yield of 1 Mt TNT (4.18×10^{15} J). Three types of nuclear explosions can be distinguished:

- pre-contact (at some distance from the surface);
- contact (at the surface);
- embedded (beneath the surface).

Under the conditions of the vacuum of space, the fraction of energy p transmitted by the nuclear explosion to an object in a pre-contact or contact explosion is very low, not exceeding 0.1 for a megaton-class nuclear device [9]. The fraction p increases appreciably even for a mildly embedded explosion, which could be realized through a preliminary collision of the asteroid with an impactor [10, 11].

We assumed in our study that the explosion occurs at a depth of 3–5 m, somewhat exceeding the dimensions of the nuclear device. A central source (a region of vaporized material of a barrier adjacent to the explosion) is formed during the course of the nuclear explosion under the action of the X-ray emission and the impact of matter from the nuclear device. This material, which is under high pressure, accomplishes the body's work. The shape of the boundary of this region is close to the surface of a spherical segment, and it is formed by the propagating thermal wave and then the shock wave; the latter forms a thin disk of vaporized rock that narrows toward the edges and has a radius that somewhat exceeds the radius of the zone of soft X-ray emission. Since the depth exceeds the size of the nuclear device, the X-ray emission is partially or fully screened. When the depth exceeds the radius of the thermal wave, the shock one is not appreciably weakened due to radiation, and the intensity of the gas-dynamical processes associated with the ejection of matter from the central source is appreciably lowered.

At early times in the process, the transfer of the energy of the nuclear explosion to the barrier is carried out mainly by X-rays. The energy of the explosion is absorbed by the material making up the nuclear device, which is heated to tens of millions of degrees and expands, simultaneously becoming a source of intense X-ray radiation. The radiation (which makes up about 90% of the total energy of the nuclear explosion) essentially completely leaves the source over about 100 ns.

The radiation heats the adjacent layer of matter in the barrier, whose thickness is determined by the mean free path of the radiation, to temperatures of order several million degrees. As the temperature of the heated layer grows, the mean free path increases, which, in turn, makes it possible to heat the following layer of matter. Due to the strong temperature dependence of the mean free path of the radiation, a thermal front forms, which separates the heated and cool material. At a temperature of several million degrees, the mean free path of the radiation in a solid body with normal density is comparable to the size of the heated region, equalizing the temperature inside the thermal wave.

As the thermal wave propagates, the temperature of the heated matter decreases, and hydrodynamical motions begin to become more important in the development of the explosion. With time, the shock that forms inside the thermal wave overtakes the wave front. Further, the main mechanism transferring energy to the matter is the propagation of this strong shock.

In contrast to the thermal wave, in which the motion of the medium is not important, the density of the matter and the velocity of its motion vary in a jump-like fashion at the shock front, and the rock undergoes various thermodynamical transformations: ionization, dissociation, vaporization, melting, and thermal decomposition of the minerals making up the rock. The radius of the vaporization zone for granite in the case of an embedded 1-Mt nuclear explosion is 15 m, and the mass of the ionized and vaporized rock is 7×10^7 kg. The corresponding parameters for the zone where melting occurs are 26 m and 1.2×10^8 kg. Since the pressure in the rock remains appreciable in this case (more than 40 GPa), the role of shear stresses is small, and the medium behaves similar to a compressible fluid, with its stress state determined purely by the pressure.

Further, the parameters of the wave are reduced, and the influence of the strength properties of the rock become important. For rock such as granite, this influence begins to be manifest when the pressure in the shock front is 20 to 40 GPa. The zone of polymorphic phase transitions corresponds to roughly this same pressure. Phase transitions and the relationship between stresses and the deformation state characteristic of a rigid medium mean that the shock front is disrupted, and the shock degenerates into a compression wave with a continuous distribution of parameters.

While the energy dissipation in the shock occurs in the presence of irreversible loading of the medium and is determined by the parameters of the front, the energy dissipation in the compression wave is associated with energy losses to inelastic deformation

and destruction of the medium. After the passage of the shock, an element of the medium expands in accordance with isentropic unloading. Depending on the entropy acquired during the passage of the shock, particles can undergo full or partial vaporization, melting, and thermal decomposition during this unloading. Having specified a reference point for the entropy and determined the entropy of a rock particle and the critical entropy of each component of the rock, it is possible to determine its state after the passage of the shock front and the subsequent phase of unloading.

This process is determined by macroeffects of the action of the nuclear explosion on the barrier.

An *explosion cavity* forms as a consequence of the densification of the rock under the action of the explosion and the compression shock. Empirical relations give a radius of this cavity of $R_1 \approx 40$ m for a megaton explosion (all radii are measured from the center of the explosion).

A *fragmentation zone* with a radius of $R_2 \approx (1.5-3)R_1 \approx (60-120)$ m adjoins the explosion cavity, where the barrier is fragmented into rubble and dust, and the characteristic size of the debris does not exceed 10 cm.

In a *zone of intense fracturing* with a radius of $R_3 \approx (3-5.5)R_1 \approx (120-220)$ m, there is volumetric and shear destruction of the granite under the action of the compression wave and unloading, and fractures associated with local weakening of the rock form. The maximum degree of fracturing reaches 4–6 new fractures per meter, and the characteristic size of the debris at the outer boundary of this zone can reach 10 m—the maximum admissible radius from the point of view of safety for the Earth. A megaton explosion is able to break up a granite asteroid with a diameter of up to 220 m into comparatively safe fragments. The radius of the zone of intense fracturing is proportional to the square root of the cube of the energy release in the nuclear explosion; therefore, having determined the size of the asteroid and the material of which it is made, it is possible to estimate the power of the nuclear charge that is required to fully disintegrate the asteroid.

Recall that our estimate of the radius of the zone of fragmentation into safe debris was obtained assuming a monolithic granite asteroid. In most real cases, intrinsic fracturing of the asteroid is developed by the nuclear explosion, increasing the zone of effective fragmentation. On the contrary, this zone is smaller than the estimate given above in rare cases of metallic asteroids.

If the size of an asteroid exceeds the size of the fragmentation region, the remaining part of the asteroid will only be subject to elastic deformation. However, the nuclear explosion will transmit an impulse to

the undestroyed part of the asteroid, changing its trajectory and making possible avoidance of a collision with the Earth.

The fraction of the energy of the nuclear explosion in gas-like products is up to 7–20%, giving rise to acceleration and decompaction of the destroyed rock, as well as a filtration flow of gas-like products through the zone of destruction.

Let us summarize the information presented in this section.

- When $D < 25$ m, the asteroid will be completely destroyed, and be transformed into gas and rapidly solidifying drops of fluid. The velocities of particles relative to the asteroid \mathcal{A} will be great enough (of order km/s) that they will virtually all move away from the collisional orbit.
- When $25 < D < 200$ m, the part of the asteroid that is adjacent to the charge ($\approx 10^8$ kg) behaves as described above. The remainder of the asteroid is broken up into fragments with diameters not exceeding 10 m.

3. REGION OF INITIAL DATA

We will now determine the region of initial data for the collection of fragments. We assumed $D = 200$ m, so that the asteroid is completely destroyed into fragments up to 10 m in size. The number of large fragments is $N \sim 10^4-10^5$. We are interested in the trajectories of the fragments right up to the time when they subsequently approach the Earth. For our estimates to have high statistical significance, we adopted $N = 10^5$ in these computations. We neglected non-gravitational forces, so that the trajectory of a fragment does not depend on its mass, only its initial position and velocity are important. Without loss of accuracy, we can assume that the initial position coincides with the position of \mathcal{A} at the moment of the explosion. The velocities of the fragments can be treated like random quantities, with full information about these velocities described by a distribution function, or a probability density, which is more convenient for computations. This probability density is unknown, but we can use a plausible representation for our purposes.

Let $\mathcal{O} = Oxyz$ be a non-rotating heliocentric coordinate system, and $\mathcal{O}_1 = O_1x_1y_1z_1$ an auxiliary non-rotating coordinate system. At the moment of the explosion t_0 , the coordinate origin O_1 coincides with \mathcal{A} . The x_1 axis is directed tangent to the heliocentric trajectory of \mathcal{A} , and the orientation of the y_1 and z_1 axes is arbitrary. The velocity of the point O_1 in the \mathcal{O} system is constant and equal to $\mathbf{v}_{\mathcal{A}}$, which is

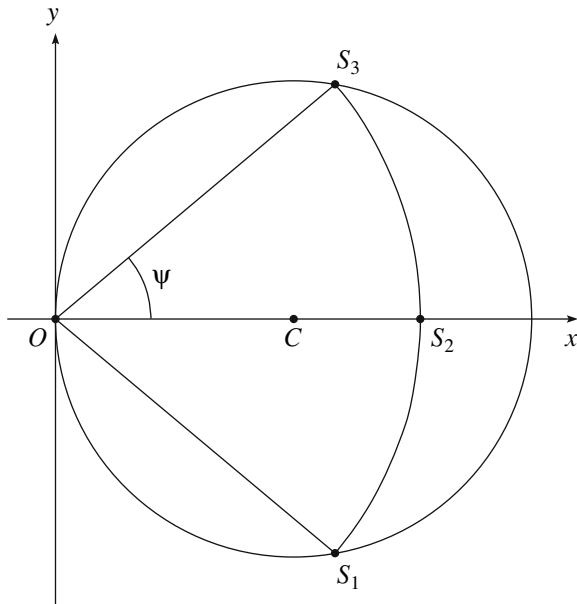


Fig. 1. Cross section of a spherical asteroid made by a plane passing through its center C . O is the center of the explosion, the arc $S_1S_2S_3$ is a section of a circle of radius $r \leq D = 2R$ with its center at O , $OC = R$, and $OS_k = r$.

the velocity of \mathcal{A} at time t_0 . The initial velocity vector of the fragments in the \mathcal{O}_1 system can be determined using the spherical coordinates v, φ, λ :

$$\begin{aligned} v_x &= v \cos \varphi, & v_y &= v \sin \varphi \cos \lambda, \\ v_z &= v \sin \varphi \sin \lambda. \end{aligned} \quad (1)$$

Let us construct probability densities for the random quantities v, φ, λ . All these values are presented in SI units if not indicated otherwise.

3.1. Speed

According to the data of [12], the speeds acquired by the particles depend on the distance r to the center of the explosion approximately in accordance with the power law

$$v = Ar^{-\sigma}, \quad r = A^{1/\sigma} v^{-1/\sigma}. \quad (2)$$

For $r > 25$ (recall that we are not interested in the near zone), we can adopt $\sigma = 1.72$, $A = 0.980 \times 10^6$.

We will now construct the distribution for the random quantity v . According to (2), it is sufficient to find the distribution of the random quantity r . Since the depth of the charge does not exceed 5 m, we can assume that the radii are measured from some point O at the surface of a sphere representing the surface of the spherical asteroid (Fig. 1). The set \mathcal{S} of points of the asteroid with $r = \text{const}$ ($0 \leq r \leq 2R = D$), forms part of a sphere with radius r forming a cut-out cone

with half opening-angle $\psi = \angle S_2OS_3$. It is natural to suppose that the probability distribution $f(r)$ for r is proportional to the area $S(r)$ of the surface \mathcal{S} .

It can easily be shown that the points S_1, S_3 of intersection of the two circles in Fig. 1 have the abscissa $r^2/(2R)$:

$$\cos \psi = \frac{r}{2R},$$

$$S(r) = 2\pi r^2(1 - \cos \psi) = 2\pi r^2 \left(1 - \frac{r}{2R}\right),$$

so that

$$\begin{aligned} f(r)dr &= \frac{3}{4\pi R^3} S(r)dr = \frac{3r^2}{2R^3} \left(1 - \frac{r}{2R}\right) dr, \\ 0 &\leq r \leq 2R. \end{aligned}$$

Since the right-hand side of (2) falls off, the distribution of the random quantity v is determined by the equality

$$f(r)dr = -f_1(v)dv,$$

so that

$$\begin{aligned} f_1(v) &= \frac{3}{2\sigma R^3} A^{3/\sigma} v^{-(3+\sigma)/\sigma} \\ &\times \left(1 - \frac{1}{2R} A^{1/\sigma} v^{-1/\sigma}\right), \\ \frac{A}{(2R)^\sigma} &\leq v < \infty. \end{aligned} \quad (3)$$

We can simplify the distribution function for the speed by introducing the new dimensionless random quantity ξ :

$$\begin{aligned} \xi &= \frac{1}{2R} A^{1/\sigma} v^{-1/\sigma}, \\ v &= \frac{A}{(2R)^\sigma} \xi^{-\sigma}, \quad dv = -\frac{A\sigma}{(2R)^\sigma} \xi^{-1-\sigma} d\xi. \end{aligned} \quad (4)$$

By definition, taking into account the monotonic dependence of v on ξ ,

$$-f_1(v)dv = f_2(\xi)d\xi,$$

whence

$$f_2(\xi) = 12\xi^2(1 - \xi), \quad 0 \leq \xi \leq 1, \quad (5)$$

which corresponds to a standard B distribution [13] with $\lambda_1 = 3$, $\lambda_2 = 2$, $B(\lambda_1, \lambda_2) = 1/12$.

The distribution function for the random quantity ξ can easily be found:

$$F_2(\xi) = \xi^3(4 - 3\xi), \quad 0 \leq \xi \leq 1. \quad (6)$$

We can now find the moments of the speed distribution

$$\int_{A(2R)^{-\sigma}}^{\infty} v^n f_1(v)dv \quad (7)$$

$$\begin{aligned}
 &= \frac{A^n}{(2R)^{n\sigma}} \int_0^1 \xi^{-n\sigma} f_2(\xi) d\xi \\
 &= \frac{12A^n}{(2R)^{n\sigma}} \int_0^1 \xi^{2-n\sigma} (1-\xi) d\xi.
 \end{aligned}$$

With $\sigma = 1.72$, there is only one first-order moment; i.e., the mean speed

$$\bar{v} = \frac{3 \times 2^{2-\sigma} A}{(3-\sigma)(4-\sigma)R^\sigma} = 444, \tag{8}$$

where the numerical values of A , R , and σ have been substituted.

As a check, we also estimated \bar{v} in another way. Let E be the energy of the explosion, $E_0 = pE$ the portion of this energy that is transformed into the kinetic energy of all the fragments (solid, liquid, and gas), with $0 < p < 1$, and $M = \pi \rho D^3/6$ the mass of the asteroid. The kinetic energy of the collection of fragments E_0 is equal to half their total mass times the square of the mean speed \bar{v} , so that

$$\bar{v} = \sqrt{\frac{2pE}{M}}.$$

Setting $p = 0.25$, in accordance with [10],

$$E = 4.18 \times 10^{15}, \quad E_0 = 1.045 \times 10^{15},$$

$$M = 1.048 \times 10^{10}, \quad \bar{v}^2 = 19.9 \times 10^4, \quad \bar{v} = 446,$$

which essentially coincides with (8).

In our computations, we used a random-number generator corresponding to the distributions (5), (6). As is known [14, Section 1.2], [15, Section 3.2], this requires the inversion of the function (6), which is strictly growing in the interval $[0, 1]$; we must find the single root of the following fourth-order equation in this interval:

$$3\xi^4 - 4\xi^3 + \eta = 0, \tag{9}$$

where η is a known number from this interval. When η is equal to zero or unity, ξ is also equal to zero or unity. When $0 < \eta < 1$, we can proceed in two ways.

First, we can use methods of computer algebra, which can provide an explicit expression for the roots of a fourth-order equation, and choose the real root that lies between zero and unity. An elementary inspection of (9) shows that it has two real roots, one of which is located between zero and unity, and the other exceeding unity.

Second, we can find the solution iteratively, writing (9) in one of two forms:

$$\begin{aligned}
 \xi &= g(\xi), \quad \text{with } 0 < \xi \leq 1/2, \tag{10} \\
 0 &< \eta \leq 5/16,
 \end{aligned}$$

$$\begin{aligned}
 \zeta &= g_1(\zeta), \quad \text{with } 1/2 < \zeta < 1, \tag{11} \\
 5/16 &< \eta < 1, \quad \zeta = 1 - \xi, \quad 0 < \zeta < 1/2.
 \end{aligned}$$

Here,

$$\begin{aligned}
 g(\xi) &= \sqrt[3]{\frac{\eta}{4}} \left(1 - \frac{3}{4}\xi\right)^{-1/3}, \\
 g_1(\zeta) &= \sqrt{\frac{1-\eta}{6-8\zeta+3\zeta^2}}.
 \end{aligned}$$

We calculate the derivatives

$$g'(\xi) = \frac{1}{4} \sqrt[3]{\frac{\eta}{4}} \left(1 - \frac{3}{4}\xi\right)^{-4/3},$$

$$g'_1(\zeta) = \sqrt{1-\eta} (4-3\zeta)(6-8\zeta+3\zeta^2)^{-3/2},$$

$$g''_1(\zeta) = 6\sqrt{1-\eta} (1-\zeta)(5-3\zeta)(6-8\zeta+3\zeta^2)^{-5/2}.$$

It is obvious that $g'(\xi)$ has its maximum value when $\xi = 1/2$ and $\eta = 5/16$. Since $g''_1(\zeta) > 0$, $g'_1(\zeta)$ acquires its largest value when $\zeta = 1/2$ and $\eta = 5/16$. Consequently, the first derivatives in the integrated intervals are restricted:

$$0 < g'(\xi) \leq \frac{1}{5}, \quad 0 < g'_1(\zeta) \leq \frac{5}{11}, \tag{12}$$

which implies convergence of the interactive process

$$\xi_{n+1} = g(\xi_n), \quad \zeta_{n+1} = g_1(\zeta_n), \tag{13}$$

when $\xi_0 = 0$ and $\zeta_0 = 0$.

We used the iterative method in our computations.

3.2. Direction of the Velocity

As is described above, the center of the explosion is located at a depth of about 3–5 m. The impacter hits the asteroid from the rear (if the asteroid is hit as it is moving away from the Earth). Therefore, practically all the fragments move forward. More precisely, their velocity vectors form a narrow angle with the velocity vector of \mathcal{A} . Backward-moving particles of matter are transformed into ionized gas, and their behavior is not important for our purposes. For simplicity, we took the directions of the particle velocities to be uniformly distributed in a hemisphere with its pole corresponding to the velocity vector \mathcal{A} . This is not completely correct, as was shown in [12], however, the non-uniformity of this distribution and its dependence on the speed does not exceed 50%, and can be neglected at this stage. Thus, the angle distribution obeys the law

$$\begin{aligned}
 f_3(\varphi) &= \sin \varphi, \quad f_4(\lambda) = 1/(2\pi), \tag{14} \\
 \varphi &\in [0, \pi/2], \quad \lambda \in [0, 2\pi].
 \end{aligned}$$

Accordingly,

$$F_3(\varphi) = 1 - \cos \varphi, \quad F_4(\lambda) = \lambda/(2\pi). \tag{15}$$

The inverse functions of F_3 and F_4 are elementary. If we denote $F_3(\varphi) = \beta$ and $F_4(\lambda) = \gamma$, then

$$\varphi = \arccos(1 - \beta), \quad \lambda = 2\pi\gamma. \quad (16)$$

Note that, if the intervention occurs when the asteroid is approaching the Earth, the fragments should move backwards (the intervention acts opposite to the direction of motion of the asteroid). Formula (14) remains valid when the third relation is replaced by $\varphi \in [\pi/2, \pi]$. The distribution for λ does not change. Formulas (15) and (16) for φ become

$$F_3(\varphi) = -\cos \varphi, \quad \varphi = \pi - \arccos \beta. \quad (17)$$

4. TRAJECTORIES OF THE FRAGMENTS

Let an asteroid moves along an orbit with the following characteristics.

- \mathcal{A} passes near the Earth, having a local minimum in the distance r_1 from its center at time t_1 , where r_1 is comparable to the radius of the Moon's orbit.
- After this encounter, the trajectory of \mathcal{A} corresponds to a resonance return orbit [16–18]. This means that the period for the motion of \mathcal{A} around the Sun in years becomes nearly exactly equal to q_1/q_2 , where q_1 and q_2 are small integers. The asteroid returns to the Earth at roughly the same date at an epoch t_2 , with $t_2 - t_1 = \tau$, where $\tau = q_1$ (in years), or q_2 (in periods of \mathcal{A}). We assumed that the nominal orbit passes a local minimum of the distance r_2 from the center of the Earth at the time t_2 , where r_2 is less than the radius of the Earth.

A nuclear charge is detonated at some epoch t_0 in a small vicinity of t_1 in order to prevent a subsequent collision of the asteroid with the Earth. Let us consider the trajectories of the debris from t_0 to t_3 , where t_3 is only slightly greater than t_2 , using numerical simulations.

We chose a trajectory leading to collision from the region of possible motions of the asteroid Apophis, derived using observations up to 2009, for which $q_1 = 7$ and $q_2 = 6$.

An object in this orbit passes at a distance of 36 830 km from the center of the Earth on April 13, 2029, and passes at a distance of 3613 km from the center of the Earth on April 13, 2036, essentially corresponding to a collision. We took the size of the asteroid in our simulations to be $D = 200$ m, so that the object can be taken to be fully broken up into fragments with diameters of up to 10 m. We took the number of fragments to be $N = 10^5$.

We considered six times during the explosion:

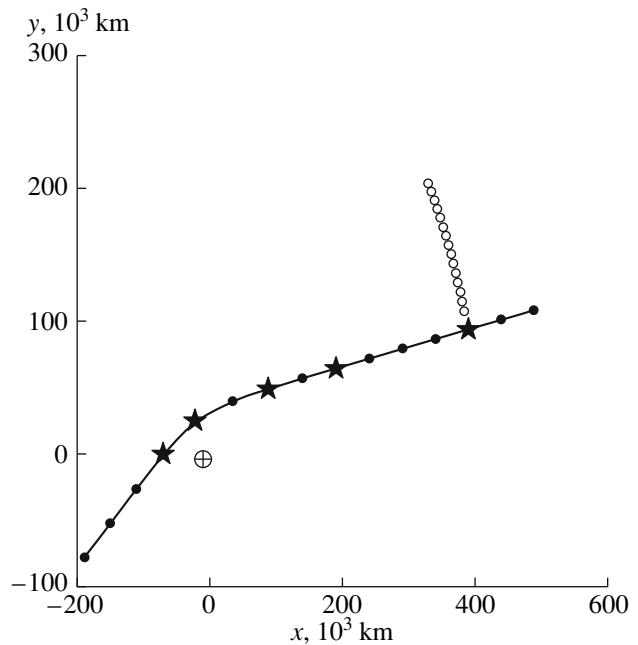


Fig. 2. Considered burst times of the asteroid.

- 1) 2 hours 34 minutes before the encounter of 2029;
- 2) ten minutes before the encounter of 2029;
- 3) 4 hours 38 minutes after the encounter of 2029;
- 4) 9 hours 26 minutes after the encounter of 2029;
- 5) 19 hours after the encounter of 2029;
- 6) 4 hours before the encounter of 2036.

The stars in Fig. 2 show the positions of the asteroid at these times (apart from the last time) in a geocentric coordinate system projected onto the plane of the equator. The solid curve shows the orbit of the asteroid, the black dots the positions of the asteroid in its orbit in steps of 0.1^d , and the circles the positions of the Moon at the same times. The Earth is shown by the circled plus sign.

The force model used in the simulations included the influence of the large planets, Pluto, the Moon, the oblateness of the Earth, and relativistic effects from the Sun. Our analysis of the orbital evolution of the fragments was carried out using the “IDA” program package developed at the Scientific Research Institute of Applied Mathematics and Mechanics of Tomsk State University, intended for studies of asteroid dynamics [19, 20].

Estimates of consequences of the explosion

Year	N_{tyg}	N_{coll}	d_{min} , km	N_{tyg}	N_{coll}	d_{min} , km	N_{tyg}	N_{coll}	d_{min} , km
	I			II			III		
2029	99 871	0	11 647	94 071	3	1183	0	0	—
2030	45	1	4068	90	9	630	0	0	—
2031	38	2	1012	87	9	1184	0	0	—
2032	24	1	408	82	8	321	0	0	—
2033	23	0	6580	81	7	1081	2	0	136 708
2034	23	0	6567	82	6	235	6	0	38 273
2035	25	2	348	81	6	1183	42	1	4554
2036	119	4	674	245	12	493	2	0	88 861
2037	187	8	1372	217	8	1182	0	0	—
2038	81	0	8131	124	5	395	1	0	179 212
2039	45	0	7120	91	5	1180	0	0	—
	IV			V			VI		
2029	44	0	94 045	0	0	—	0	0	—
2031	1	0	101 809	0	0	—			
2032	2	0	11 994	1	0	116 136	0	0	—
2033	0	0	—	2	0	23 635	0	0	—
2034	12	1	3135	6	0	34 935	0	0	—
2035	104	2	2032	43	1	4732	0	0	—
2036	138	5	829	43	2	1211	1068	644	127
2037	0	0	—	0	0	—	0	0	—
2038	8	1	3725	0	0	—	0	0	—

We carried out simulations of the explosion for each of the times indicated above. Namely, the initial position of each fragment was taken to coincide with the position of \mathcal{A} , and its velocity was chosen randomly in accordance with the distribution (3), (16), (17). Further, the evolution of each fragment was studied numerically using the above force model. The table presents for each explosion the explosion number (corresponding to the numeration of the explosion times listed above), the number of particles passing through the gravitational sphere of the Earth in various years N_{tyg} and the corresponding number of particles colliding with the Earth N_{coll} , and the minimum distance from the center of the Earth d_{min} in various years. The total number of fragments was 100 000 in all cases.

As expected, the most dangerous explosion is the one that occurs before the encounter of 2036 (VI), which leads to the fragments (hundreds) falling onto the Earth. The majority of the remaining explosions lead to an appreciable number of fragments passing through the gravitational sphere of the Earth, but with only a few colliding with the Earth in various years. Explosion of the object immediately after the encounter of 2029 (III) gives the best result, since this leads to only one fragment colliding with the Earth (in 2035).

5. DANGER OF RADIOACTIVE IMPACTS

The overall activity Q of matter an hour after a megaton nuclear explosion is extremely high, 300 GCi, but falls rapidly with time. The decay rate

for a collection of a large number of isotopes varies in accordance with a complex law, but can to good approximation be taken to be a power law in the interval from several minutes to several years [21]:

$$Q = qt^{-1.2}, \quad (18)$$

where $q = 5.5$ if the activity is measured in MCi and time is given in years.

As expected, the explosion preceding the collision (VI) leads to hundreds of highly radioactive fragments impacting the Earth. This option must be considered completely unacceptable: a swarm of bodies with an overall radioactivity of 360 MCi falls onto the Earth. Even if this matter were uniformly distributed over the entire surface of Africa, this yields 12 Ci/km². It is currently usual to consider acceptable levels of radiative contamination to be no more than 5 Ci/km².

Explosion not long before the encounter (I and II) is not catastrophic, but much more dangerous than an explosion after the encounter.

The most favorable case is III, when only one fragment falls onto the Earth six years after the explosion:

$$t = 6 \text{ yrs}, \quad Q = 0.64 \text{ MCi.}$$

If we take the activity Q_0 of the fragment that falls onto the Earth in 2035 to be $10^{-4}Q$, then $Q_0 = 64 \text{ Ci}$. Scattering of the fragment material in the atmosphere and precipitation of the ablation products over an area of more than 13 km² would automatically eliminate any radiation hazard.

It stands to reason that it would be best to choose a time for the explosion that guarantees that all fragments will fly past the Earth. However, this is unlikely to be possible, given the probabilistic character of the initial velocities of the fragments.

6. CONCLUSION

We have considered the destruction of a hazardous asteroid using a nuclear charge long before its predicted impact on the Earth. The aim of our study was to demonstrate the fundamental possibility (or impossibility without dangerous consequences) of this means of defense against asteroid hazard. Therefore, we assumed an idealized situation: a spherical asteroid that is destroyed with the formation of 10^5 fragments, and a simple distribution function for the velocity components of the fragments. The results show that this approach is realistic. When the explosion takes place after an encounter, 1–9 fragments fall onto the Earth after 10 years. Over this time, their radioactivity has been reduced to acceptable levels. Carrying out the explosion a short time before the encounter is completely unacceptable: an enormous

number of highly radioactive fragments would then fall onto the Earth.

It stands to reason that the real destruction of a specific hazardous asteroid would require substantially more careful work. In particular, it would then be necessary to reject this idealization of the problem. This is work for the future.

ACKNOWLEDGMENTS

This work was supported by the D.I. Mendeleev Scientific Foundation of Tomsk State University (project 8.1.54.2015), St. Petersburg State University (grant 6.37.341.2015), and the Russian Foundation for Basic Research (grant 14-02-00804).

REFERENCES

1. B. M. Shustov, L. V. Rykhlova, Yu. P. Kuleshov, Yu. N. Dubov, K. S. Elkin, S. S. Veniaminov, G. K. Borovin, I. E. Molotov, S. A. Naroenkov, S. I. Barabanov, V. V. Emel'yanenko, A. V. Devyatkin, Yu. D. Medvedev, V. A. Shor, and K. V. Kholshchevnikov, *Solar Syst. Res.* **47**, 302 (2013).
2. A. N. Vereshchaga, V. G. Zagrafov, and A. K. Shantenko, *Vopr. At. Nauki Tekh., Teor. Prikl. Fiz.*, No. 3/1, 3 (1994–1995).
3. A. N. Vereshchaga, V. G. Zagrafov, and A. K. Shantenko, in *Space Protection of the Earth SPE-96* (Chelyabinsk-70, Snezhinsk, 1996), p. 82.
4. A. V. Tukmakov, Bachelor's Final Work (Higher School Economics, Moscow, 2013).
5. B. M. Shustov and L. V. Rykhlova, *Asteroid-Comet Hazard: Yesterday, Today, Tomorrow* (Fizmatlit, Moscow, 2013) [in Russian].
6. D. Perna, M. A. Barucci, and M. Fulchignoni, *Astron. Astrophys. Rev.* **21**, 65 (2013).
7. A. V. El'kin and L. L. Sokolov, in *Asteroid Hazard-95* (MIPAO, ITA RAN, St.-Petersburg, 1995), Vol. 2, p. 41.
8. V. V. Emelyanenko, *Planet. Space Sci.* **118**, 302 (2015).
9. V. N. Arkhipov, V. A. Borisov, A. M. Budkov, V. V. Val'ko, A. M. Galiev, O. P. Goncharova, I. M. Zaikov, B. V. Zamyshlyaev, A. M. Knestyapin, V. S. Korolev, V. D. Kuzovlev, E. V. Makarov, I. Yu. Seliverstov, G. I. Semenov, V. V. Smaznov, E. I. Smirnov, and O. N. Ushakov, *The Mechanical Effect of Nuclear Explosions* (Fizmatlit, Moscow, 2003) [in Russian].
10. V. S. Sazonov, *Ekol. Vestn. Nauch. Tsentrov ChES* **3**, 118 (2013).
11. S. A. Meshcheryakov and Yu. M. Lipnitskii, *Tech. Phys.* **60**, 26 (2015).
12. *The Effect of Nuclear Weapons*, Ed. by H. L. Brode, Collection of Articles (Mir, Moscow, 1971) [in Russian].

13. A. S. Shmyrov and V. A. Shmyrov, *The Theory of Probabilities* (VVM, St.-Petersburg, 2012) [in Russian].
14. S. M. Ermakov and G. A. Mikhailov, *Statistical Modelling* (Nauka, Moscow, 1982) [in Russian].
15. A. A. Borovkov, *The Theory of Probabilities* (Editorial URSS, Moscow, 1999) [in Russian].
16. S. R. Chesley, in *Asteroids, Comets, Meteors*, Ed. by L. Daniela, M. Sylvio Ferraz, and F. J. Angel (Cambridge Univ. Press, Cambridge, 2006), p. 215.
17. L. L. Sokolov, A. A. Bashakov, and N. P. Pit'ev, *Solar Syst. Res.* **42**, 18 (2008).
18. L. L. Sokolov, A. A. Bashakov, and N. P. Pit'ev, *Solar Syst. Res.* **43**, 319 (2009).
19. L. E. Bykova and T. Yu. Galushina, *Izv. Vyssh. Uchebn. Zaved., Fiz.* **52** (10/2), 12 (2009).
20. L. E. Bykova, T. Yu. Galushina, and A. P. Baturin, *Izv. Vyssh. Uchebn. Zaved., Fiz.* **55** (10/2), 89 (2012).
21. V. D. Burlakov and N. N. Tulinov, *The Effects of Nuclear Weapons* (Voenizdat, Moscow, 1960) [in Russian].

Translated by D. Gabuzda